



(RESEARCH ARTICLE)



Virtual high-throughput screening (VHTS), three-dimensional quantitative structure-activity and relationship (3D-QSAR) and molecular docking studies of novel phyto-inhibitors of topoisomerase II alpha

Olawole Y. Adeniran *, Ayorinde O. Metibemu and Samuel O. Boboye

Department of Biochemistry, Adekunle Ajasin University, Akungba-Akoko, Ondo State, Nigeria.

GSC Biological and Pharmaceutical Sciences, 2021, 15(02), 072–082

Publication history: Received on 27 March 2021; revised on 30 April 2021; accepted on 03 May 2021

Article DOI: <https://doi.org/10.30574/gscbps.2021.15.2.0099>

Abstract

Topoisomerase II alpha catalyses and guides the unknotting of DNA by creating double transient breaks in the DNA using a conserved tyrosine as the catalytic residue. Topoisomerase II alpha has been shown to be overexpressed in numerous types of cancers and it is a target for multiple chemotherapeutic agents. Many DNA topoisomerase inhibitors have been identified from natural sources and have been reviewed in many reports as anticancer agents. In the present study, a total of 240 phytochemicals characterized from four reported anticancer plants (*Anacardium occidentale*, *Andrographis paniculata*, *Cannabis sativa* and *Tinospora cordifolia*) were obtained from literatures and screened against the binding pocket of topoisomerase II alpha. From the pool of phytochemicals only 7-o-methylcyanidin, 20-betaecdysone, Andropanoside and Palmatoside-G qualified as Phyto-compounds with good oral bioactivity when subjected to the Lipinski's rule of five. Bioassay data containing the IC₅₀ of compounds screened against topoisomerase II alpha was used to generate a regression model using the 3D-QSAR techniques. A very viable model with R² = 0.954, adjusted R² = 0.908, Pearson R = 0.977, cross validation Q² = 0.851, Standard Error of Estimate = 0.125, F = (20.803, p < 0.05) and Durbin-Watson constant = 1.613 was obtained. The 3D-QSAR result shows that Andropanoside and 20-betaecdysone may be better inhibitors of topoisomerase II alpha catalytic site than the standard drug, Etoposide. To further confirm this, the molecular interactions of Andropanoside and 20-betaecdysone were compared to those of Etoposide using the ligand interaction interface of Maestro environment.

Keywords: Cancer; Topoisomerase II alpha; DNA replication; Etoposide; Phytochemicals; Three-Dimensional Quantitative Structure-Activity and Relationship (3D-QSAR).

1. Introduction

Cancer is a group of diseases characterized by abnormal cells that grow and invade healthy cells in the body and is amongst the leading cause of death worldwide [1] and [2]. Cancer cells develop a degree of autonomy from signals that dictate when the cells should divide, differentiate into another cell or die and this result in uncontrolled growth and proliferation which can be fatal when allowed to continue and spread [3]. Almost all types of mammalian cells carry an inbuilt circuit, which controls their rate of cell division. This control is the key to maintain the integrity (size and shape) of the cell and the tissues. Tissues can develop to enormous sizes with lethal results for the organism if they continue to divide without any intrinsic constraint. Cancer cells divide more rapidly than normal cells. They are typically defined by their capacity to divide uncontrollably and their ability to result into a potentially fatal tumour must be a disruption in the inherent cellular circuitry controlling cell multiplication [4, 3, 5]. During cell division, DNA replicates during the S phase of the cell cycle creating twice the number of chromosomes [3]. Proteins involved in DNA replication include DNA polymerase, Helicase, DNA Topoisomerases, etc. To facilitate rapid cell division, cancer cells require higher

* Corresponding author: Olawole Y Adeniran

Department of Biochemistry, Adekunle Ajasin University, Akungba-Akoko, Ondo State, Nigeria.

topoisomerase activity and indeed these enzymes have been overexpressed in numerous types of cancers [6,7,8]. Topoisomerases are isomerase enzymes that act on the topology of DNA. In order to prevent and correct these types of topological problems caused by the double helix, topoisomerases bind to DNA and cut the phosphate backbone of either one or both the DNA strands. This intermediate break allows the DNA to be untangled or unwound, and, at the end of these processes, the DNA backbone is resealed again [9]. Topoisomerase II alpha plays a key role in DNA replication and it is a target for multiple chemotherapeutic agents [10]. It is the key target enzyme for the topoisomerase inhibitor class of anti-cancer drugs [11].

Drugs targeting topoisomerase II (Top 2) are divided into two broad classes. They are the Top 2 poisons and catalytic inhibitors [12]. Top 2 poisons lead to increases in the levels of Top 2 ratio DNA covalent complexes. Examples include etoposide, doxorubicin and mitoxantrone. The catalytic inhibitors inhibit Top 2 catalytic activity but they do not generate increases in the levels of Top 2 covalent complexes. They are thought to kill cells through elimination of its essential enzymatic activity [12] and a good example is merbarone [13]. Etoposide like other topoisomerase II poisons forms a ternary complex with DNA and the topoisomerase II enzyme, preventing the re-ligation of the DNA strands, and by doing so causes DNA strands to break [14]. Topoisomerase inhibitors have some therapeutic limitations and they exert serious side effects during cancer chemotherapy. Thus, development of novel anticancer topoisomerase inhibitors is necessary for improving cancer chemotherapy [15]. Targeting topoisomerases by small molecule inhibitors in different cancers is an interesting area of investigation. Many DNA topoisomerase inhibitors have been identified from natural sources, as reviewed in many reports regarding topoisomerase inhibitors as anticancer agents [16, 17,14, 18,19].

Many Medicinal plants such as *Albizzia lebeck*, *Tinospora cordifolia*, *Andrographis paniculata*, *Curcuma longa*, *Anacardium occidentale*, etc. have been shown to have anticancer properties [20]. The extracts from *Anacardium occidentale* have been reported to have prophylactic, anesthetic, bactericidal and insecticidal properties [21] as well as anti-tumour and antioxidant potentials. Numerous studies have provided evidence that cannabinoids from *Cannabis sativa* exhibit antitumor effects in a wide array of animal models of cancer [22, 23].

In this study, about 240 phytochemicals from four anticancer plants (*Anacardium occidentale*, *Andrographis paniculata*, *Cannabis sativa* and *Tinospora cordifolia*) obtained from literatures were screened against topoisomerase II alpha and 3D-QSAR model was generated for the identification of novel topoisomerase II alpha's inhibitors.

2. Material and methods

2.1. Data Collection and Preparation

Various phytochemicals characterized from *Argerantum conyzoides*, *Cannabis sativa*, *Andrographis paniculata* and *Tinospora cordifolia* were collected from various literatures. The 2D structures of the phyto-compounds were downloaded from Pubchem database (<http://www.rcsb.org/pdb>). Under Schrödinger-Maestro tools, the compounds were desalted and the respective 3D conformers of ligands at pH 7.0± 2.0 were generated using LigPrep tool.

2.2. Protein Preparation for Docking

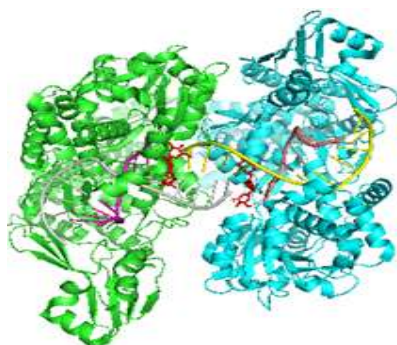


Figure 1 The 3-dimensional structure of the Human Topoisomerase II alpha receptor, complex with Etoposide and DNA strands with PDB ID: 5GWK

The 3D crystalized conformation of the topoisomerase II alpha bound to DNA double strand and Etoposide as inhibitor was downloaded from the Protein Data Bank (PDB) repository with the PDB ID of 5GWK and a crystallographic resolution of 3.18Å. Schrödinger-Maestro was used as the graphical user interface and the Protein was prepared using protein preparation wizard. The missing side-chain atoms within the protein residues and the missing loops were filled by Prime (Schrödinger). The Co-crystallized ligand, water molecules, ions and cofactors were deleted, hydrogen atoms were added, and formal charges along with bond orders were assigned to the structures. The protein has two subunits of the same amino acid sequence and composition, labeled as chain A and chain B with the Etoposide (C and D) and the DNA double strands (E and F) respectively bound to each subunit. For the purpose of ligand-protein docking, only chains B, D and E were removed. The prepared protein was loaded into maestro environment and the active site was defined using the grid box of the co-crystallized ligand X = -23.31, Y = -38.58 and Z = -59.57.

2.3. Ligand Docking

The molecular docking was carried out using GLIDE (Grid-based Ligand Docking with Energetics). The prepared compounds were subjected to glide standard precision (SP flexible) ligand docking in Glide docking module of Schrödinger-Maestro v11.1. The first few of the results from SP docking were re-docked using the extra-precision (XP) mode of Glide. The XP glide combines a powerful sampling protocol with a custom scoring function designed to identify ligand poses that would be expected to have unfavorable energies, based on well-known principles of physical chemistry. The presumption is that only active compounds will have available poses that avoid these penalties and also receive favorable scores for appropriate hydrophobic contact between the protein and the ligand, hydrogen-bonding interactions, and so on [24]. The chief purpose of the XP method was to weed out false positives and to provide a better correlation between good poses and good scores. Extra-precision mode is a refinement tool designed for use only on good ligand poses.

2.4. Validation of Docking Results

The quality of reproduction of a known crystallographic binding pose of docking can be measured by calculating the Root-Mean-Square deviation (RMSD) of the poses. The co-crystallized ligand was extracted and re-docked into its binding pocket. Using the Superposition wizard of the Schrodinger suite, the overlapping poses of the co-crystallized ligand before and after docking were compared. The Root-Mean-Square deviation (RMSD) value was also obtained. A RMSD value of not more than 2Å is commonly used as the accepted threshold for a correctly reproduced crystal pose [25].

2.5. Rule of five filters

All the compounds structures were subjected to Lipinski's rule of five. The properties of the compounds were obtained using the ADME of Schrodinger suite. Lipinski's rule of five is used to evaluate compounds for good oral bioavailability in order to be an effective drug-like compound. According to this rule, a drug-like molecule should have not more than one of the following violations: not more than five hydrogen bond donors; not more than ten hydrogen bond acceptors; molecular weight not more than 500g/mol; and Log P not more than 5 [26].

2.6. Three-Dimensional Quantitative Structure Activity Relationship (3D-QSAR)

The bioassay IC₅₀ data topoisomerase II alpha was downloaded from Pubchem-Chembl database in excel format and converted to sdf format (2-dimensional structures) using DataWarrior. The catenated output structures in sdf format were converted to 3-dimensional sdf format and opened with chemistry development kit (CDK) to generate molecular descriptors for the compounds. The descriptors generated were pretreated to reduce the descriptors to the most important ones with pretreatment software (V-WSP) and divided into training (70%) and test (30%) dataset. Using Genetic Algorithm (Roy and Mitra), the training set was screened to get the best fit variables. The output, using the R software was used to generate a model and plot different graphs including normal distribution histogram, Pearson correlation and so on. Applying it to predict the negative log of inhibitory concentration (pIC₅₀) of the test dataset validated the model and the Pearson R was determined. The equation was used to predict the half-maximal inhibitory concentration (IC₅₀) of the lead compounds.

2.7. Molecular docking and interaction

The ligand-protein molecular interaction of the compounds was generated using the Ligand interaction module of the Maestro interface. The poses of the co-crystallized ligand (Etoposide) before and after docking was compared using the superimposition tool and their interaction with the protein residues were compared.

Also, using the Ligand interaction module of the software, the interaction of the co-crystallized ligands was generated.

3. Results and discussion

Extraction and re-docking of the co-crystallized ligand (Etoposide) using Extra precision (XP) gave a glide docking score of -7.346 kcal/mol.

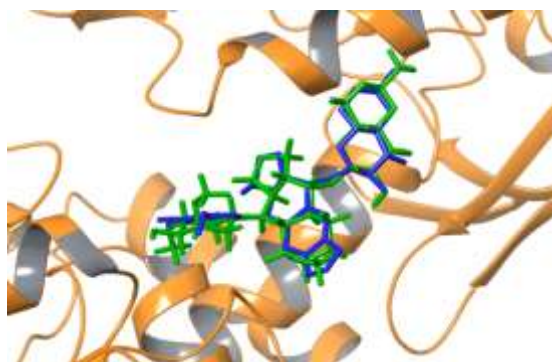


Figure 2 Showing the superposition of the co-crystallized ligand (Etoposide) before and after docking

The poses of the co-crystallized ligand (Etoposide) before and after docking was superposed using the Superposition wizard of the Schrodinger suite. The pose before docking (colour blue) and after docking (colour green) only have little difference in conformation. The RMSD value of 0.7Å (<2.0 Å) indicates a correctly reproduced crystal pose of docking.

Table 1 Showing the glide scores of the lead compounds and their plant scores

S/N	Phytochemical	ChEMBL_ID	Glide score	Plant Source
1	7-O-methylcyanidin	101765178	-10.395	<i>Anacardium occidentale</i>
2	RUTIN	5280805	-9.847	<i>Anacardium occidentale</i>
3	Luteolin-7-O-glucoside	5280637	-9.563	<i>canabis sativa</i>
4	Myricetin 7-glucoside	44259443	-9.383	<i>Anacardium occidentale</i>
5	Palmatoside B	46217668	-8.096	<i>Tinospora cordifolia</i>
6	Andropanoside	44575270	-7.9	<i>Andrographis paniculata</i>
7	Grossamide	101262727	-7.862	<i>canabis sativa</i>
8	Palmatoside C	101506923	-7.757	<i>Tinospora cordifolia</i>
9	20-beta-ecdysone	5459840	-7.713	<i>Tinospora cordifolia</i>
10	Cordifolioside A	101676711	-7.693	<i>Tinospora cordifolia</i>
11	Palmatoside G	184515	-7.665	<i>Tinospora cordifolia</i>

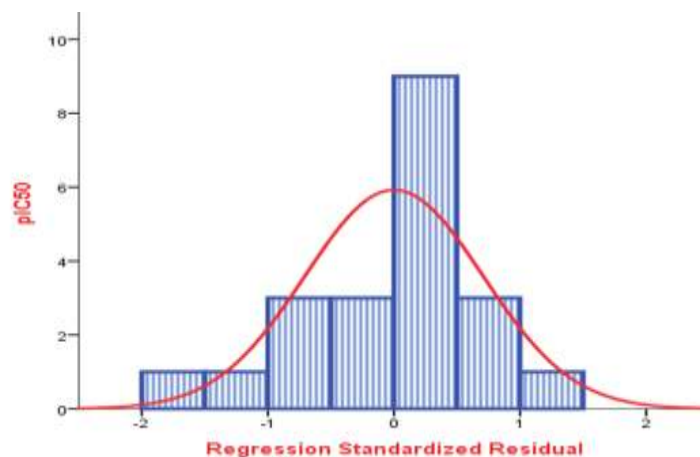
The above table shows the lead compounds which have docking (XP glide) scores above that of the co-crystallized ligand (Etoposide XP glide score = -7.346 Kcal/mol). Three of the six compounds, (7-O-methylcyanidin, Rutin and Myricetin 7-glucoside) are from *Anacardium occidentale*, two (Luteolin 7-O-glucoside and Grossamide) from *canabis sativa* and one (Andropanoside) from *Andrographis paniculata*.

Below table contains the Pharmacokinetics properties as displayed by the Schrodinger software. Hydrogen bond acceptor (HBA) and donor (HBD), molecular weight (M.W), XlogP (XlogP3) as well as the number of rotatable bonds (R.B) were selected to screen the compounds for their drug-likeness properties based on the Lipinski's rule of five. From the table, Andropanoside from *Andrographis paniculata*, 7-O-methylcyanidin from *Anacardium occidentale* and 20-beta-ecdysone and Palmatoside G from *Tinospora cordifolia* are the compounds that do not disobey more than one Lipinski's rule of five, hence they are fit as orally active drugs.

Table 2 Table the results of testing of the lead compounds as well as the co-crystallized ligand (Etoposide) with Lipinski's rule for their drug oral bioavailability

Compounds	HBA (≤ 10)	HBD (≤ 5)	R.B (≤ 10)	M.W (< 500)	XlogP3 (≤ 5)	Rule of 5 Violation
7-O-methylcyanidin	10	7	5	463.415	0	1
RUTIN	16	10	6	610.521	-1.3	3
Myricetin 7-glucoside	13	9	4	480.378	0	2
Luteolin 7-O- glucoside	11	7	4	448.38	0.5	2
Grossamide	8	5	12	624.69	4.9	2
Andropanoside	9	5	7	496.597	1.3	0
Palmatoside B	17	7	12	734.704	1	4
Palmatoside C	16	8	8	636.559	0.2	3
20-beta-ecdysone	7	6	5	480.642	0.5	1
Cordifolioside A	11	4	6	522.547	-0.1	2
Palmatoside G	10	4	5	492.521	0.1	0
Etoposide	13	3	5	588.562	0.6	2

3.1. Three-Dimensional Quantitative Structure Activity Relationship (3D-QSAR)

**Figure 3** Histogram showing the Normal distribution of the residual.

The model generated from the training set has an R^2 value = 0.954, adjusted R^2 value = 0.908, Pearson correlation = 0.977, cross validation Q^2 = 0.851, Standard Error of Estimate = 0.125, F = (20.803, $p < 0.05$) and Durbin-Watson constant = 1.613.

Equation of the model:

$$\text{Predicted pIC}_{50} = 13.787 + (1.121 * \text{geomShape}) + (14.392 * \text{FPSA-1}) + (-2.454 * \text{MDEN-23}) + (48.931 * \text{BCUTc-1}) + (-0.005 * \text{DPSA-1}) + (-1.536 * \text{MOMI-XY}) + (-0.222 * \text{LipinskiFailures}) + (-2.165 * \text{Weta1.unity}) + (0.091 * \text{PPSA-3}) + (-0.436 * \text{MDEO-12})$$

Where:

FPSA-1: PPSA-1 / total molecular surface area

MDEN-23: Molecular distance edge between all secondary and tertiary nitrogens

BCUTc-1l: Number of high lowest partial charge weighted BCUTS

DPSA-1: Difference of PPSA-1 and PNSA-1

MOMI-XY: Ratio of moment of Inertia of X and Y

LipinskiFailures: Number failures of the Lipinski's Rule of 5

Weta1.unity: Directional WHIM, weighted by unit weights

PPSA-3: Charge weighted partial positive surface area

geomShape: Petitjean geometric shape index

MDEO-12: Molecular distance edge between all primary and secondary oxygens

The histogram plot in Figure 3 shows the normality of the residuals (difference between the observed and the predicted pIC_{50}). The distribution of the residual is normal; the histogram is symmetrical and approximately bell-shaped.

Table 3 Showing the values of the experimental (Observed) pIC_{50} and the predicted pIC_{50} for the twenty compounds of the training set.

CHEMBL_ID	Observed Value		Predicted Value	
	pIC_{50}	IC_{50}	pIC_{50}	IC_{50}
2260087	5.4	3.98	5.26513	5.43
2260091	5.3	5.01	5.28792	5.15
2260081	5.39	4.07	5.43854	3.64
2259878	5.54	2.88	5.56989	2.69
116438	4.82	15.14	4.80445	15.7
2259873	5.68	2.09	5.64908	2.24
2259872	5	10	4.97339	10.64
2260083	5.4	3.98	5.26475	5.43
2259877	5.35	4.47	5.33990	4.57
2259876	5.52	3.02	5.49739	3.18
2259875	5.15	7.08	5.13940	7.26
2260092	4.8	15.85	5.00952	9.77
2260090	6.46	0.35	6.42430	0.38
2260073	5.52	3.02	5.48254	3.29
2260075	4.72	19.05	4.76226	17.29
2260088	4.82	15.14	4.85116	14.09
2260077	5.54	2.88	5.55817	2.77
2260086	4.7	19.95	4.66190	21.88
2260079	4.92	12.02	4.86587	13.61
2259642	5.13	7.41	5.13024	7.41
2260078	5.47	3.39	5.65418	2.22

Table 3 shows the values of the observed as well as the predicted pIC_{50} and the corresponding IC_{50} values for the training set used.

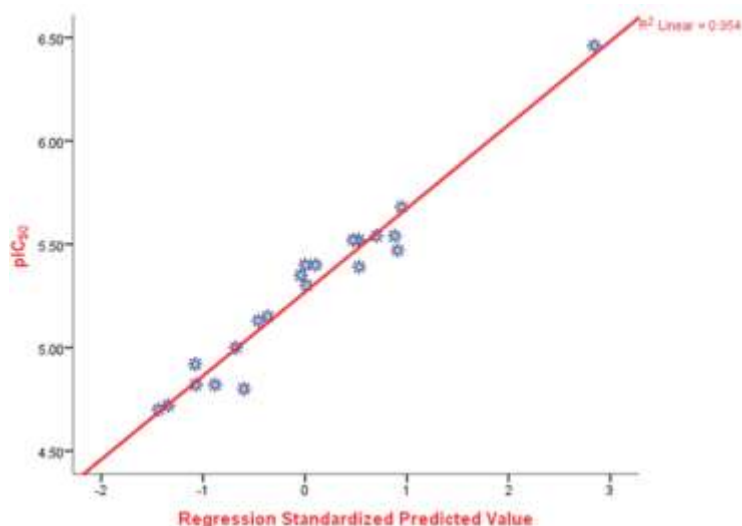


Figure 4 Plot of the observed pIC₅₀ against the predicted pIC₅₀.

The above plot shows a good linear relationship between the observed and the predicted pIC₅₀. The plot gave a Pearson R of 0.977 significant at $p < 0.05$. This shows the model accurately predict over 97% of the observed pIC₅₀

Table 4 Table showing the values of the predicted pIC₅₀ and IC₅₀ of Etoposide and the lead compounds.

Compound	Predicted pIC ₅₀	Predicted IC ₅₀
Etoposide	4.59	25.7 μ M
Andropanoside	5.29	5.12 μ M
7-O-methylcyanidin	1.20	63.1 mM
20-beta-ecdysone	5.71	1.95 μ M
Palmatoside G	4.45	35.5 μ M

The table above shows the values of the predicted pIC₅₀ values generated for the co-crystallized compound (Etoposide) and the screened lead compounds. The Predicted pIC₅₀ obtained for Etoposide (4.59) is close to some of the observed pIC₅₀ (4.66, 4.55 and 4.47) obtained from ChEMBL bioactivity with Target ID: ChEMBL1806. Andropanoside and 20-beta-ecdysone have pIC₅₀ (5.29 and 5.71 respectively) greater than that of Etoposide (4.59) while 7-O-methylcyanidin and Palmatoside G have lesser pIC₅₀ (1.20 and 4.45 respectively) than Etoposide. The higher pIC₅₀ (lower IC₅₀) seen with Andropanoside and 20-beta-ecdysone in comparison with the standard drug showed that they may be better inhibitors of the protein (Topoisomerase II alpha) than the standard drug.

3.2. Molecular interaction of the compounds

Using the ligand interaction interface of the Maestro version 11.1, the 2-dimensional interactions of Etoposide and the lead compounds were determined as shown in the figures 5a to 5c below.

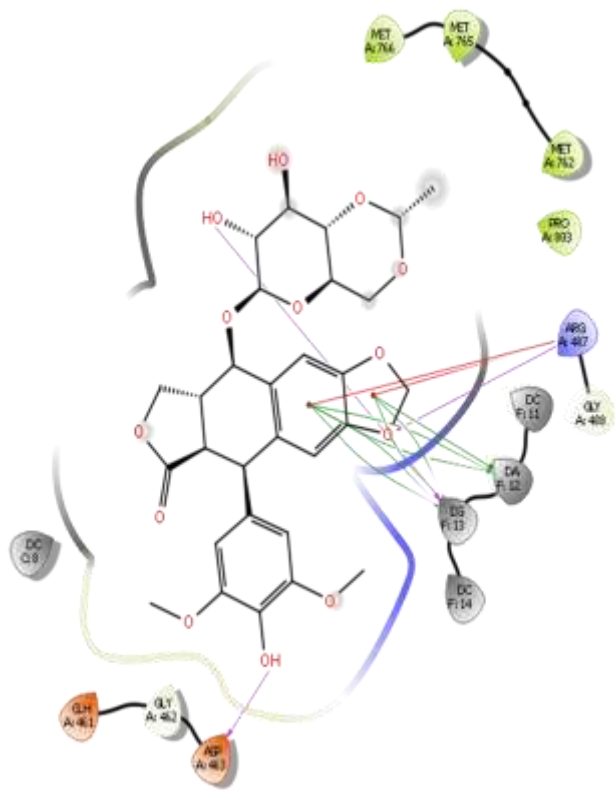


Figure 5a Showing the 2D interaction of Etoposide in its binding pocket of Topoisomerase II alpha.

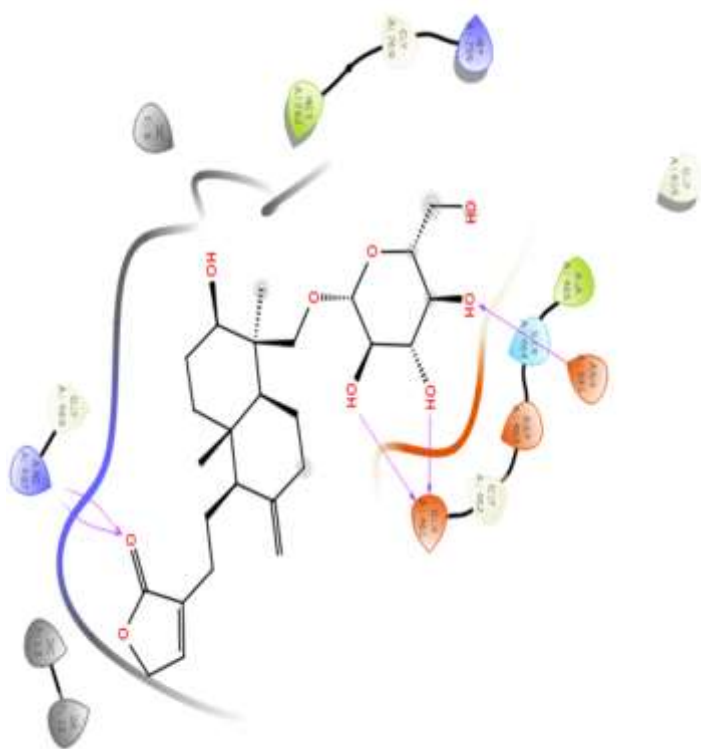


Figure 5b Showing the 2D interaction of Andropanoside in the Etoposide binding pocket of Topoisomerase II alpha.

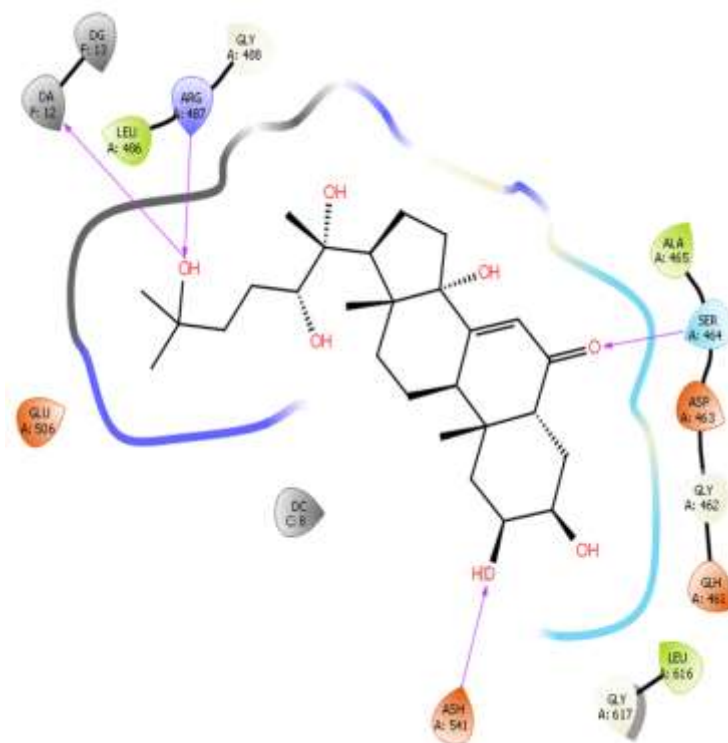
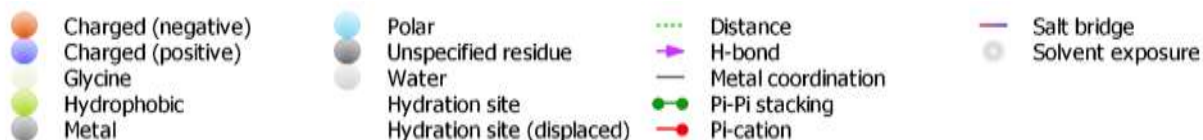


Figure 5c Showing the 2D interaction of 20-betaecdysone in the Etoposide binding pocket of Topoisomerase II alpha.



Legends (keys) to the 2D interaction of the lead compounds in the Etoposide binding pocket of Topoisomerase II alpha, the figures above (figure 5a-5c) show the molecular interaction of Etoposide and the lead compounds, and the amino acid residues and nucleotides within the Etoposide binding pocket of Topoisomerase II alpha.

Figure 5a shows the interaction of Etoposide within its binding pocket. It forms Hydrogen bonds with ARG 487, ASP 463 and DG 13, two pi-cation interactions with ARG 487 and pi-pi stacking with DG 13(deoxy guanosine) and DA 12 (deoxy adenosine). Figure 5b shows the interaction of Andropanoside. Andropanoside has 2 Hydrogen bonds with ARG 487 and GLH 461 and one Hydrogen bond with ASH 541. 20-beta-ecdysone has one hydrogen bond each with ARG 487, SER 464, ASH 541 and DA 12 as shown in figure 5c. Other residues around the binding pocket include MET 762, GLY 760, ASH 543, GLY 462, SER 464, GLY 625, MET 766 and so on.

The results obtained from the interaction of the compounds support the studies of Wendorff *et al.*, [26]. ASP 541, ASP 543, MET 762, SER 800, ARG 487, ASP 463 as well as MET 766 were reported to be important residues around the Etoposide binding pocket of the Topoisomerase II alpha-DNA complex and hence aid in the inhibition of the protein-DNA complex.

The better (higher) binding of the lead compounds when compared to that of Etoposide may be either because of the hydrogen bond they receive from ASH 541(neutral ASP) or due to the excess hydrogen bonding they have with the interacting residues and nucleotides or both. Etoposide shows 3 hydrogen bond interactions and no interaction with ASH 541 while the lead compounds (Andropanoside and 20-beta-ecdysone) have hydrogen bond interactions with ASH 541 and forms 5 and 4 hydrogen bonds respectively. Interactions with ARG 487 is common to Etoposide, Andropanoside and 20-beta-ecdysone, ASP 463 is common to both Etoposide and 7-O-methylcyanidin (7-O-methylcyanidin has 2 hydrogen bonds while Etoposide has one hydrogen bond and 2 pi-cation interactions with the residue).

4. Conclusion

Andropanoside from *Andrographis paniculata* and 20-beta-ecdysone from *Tinospora cordifolia* showed better (higher) binding energy (glide docking scores) as well as higher pIC₅₀ (lower IC₅₀) than the co-crystallized ligand. Andropanoside and 20-beta-ecdysone are potential anti-cancer compounds that can inhibit topoisomerase II alpha and may be better poisons to the protein than Etoposide.

Compliance with ethical standards

Acknowledgments

Special thanks to Damilohun S. Metibemu for technical support.

Disclosure of conflict of interest

The authors declared that they have no conflict of interest.

References

- [1] Torre LA, Bray F, Siegel RL, Ferlay J, Lortet-Tieulent J, Jemal A. Global cancer statistics, 2012. *CA Cancer J Clin.* 2015; 65: 87–108.
- [2] Torre LA, Siegel RL, Ward EM, Jemal A. Global Cancer Incidence and Mortality Rates and Trends—An Update. *Cancer Epidemiol Biomarkers Prev.* 2016; 25: 16–27.
- [3] Hejmadi M. How cancer arises. *Introduction to Cancer Biology.* Frederiksberg, Denmark: BoonBooks.com. 2010.
- [4] Hayflick L. Mortality and immortality at the cellular level. *A Review Biochemistry.* 1997; 62: 1180-1190.
- [5] Kaur S, Kaur S. Bacteriocins as Potential Anticancer Agents. *Frontiers in pharmacology.* 2015; 6: 272.
- [6] Pfister TD, Reinhold WC, Agama K, Gupta S, Khin SA, Kinders RJ, Parchment RE, Tomaszewski JE, Doroshov JH, Pommier Y. Topoisomerase I level in the NCI-60 cancer cell line panel determined by validated ELISA and microarray analysis and correlation with indenoisoquinoline sensitivity. *Mol. Cancer Ther.* 2009; 8(7): 1878-1884.
- [7] Ashour ME, Atteya R, El-Khamisy SF. Topoisomerase mediated chromosomal break repair: an emerging player in many games. *Nat. Rev. Cancer.* 2015; 15(3): 137-151.
- [8] Chen T, Sun Y, Ji P, Kopetz S, Zhang W. Topoisomerase II alpha in chromosome instability and personalized cancer therapy. *Oncogene.* 2015; 34(31): 4019-4031.
- [9] Champoux JJ. DNA topoisomerases: structure, function, and mechanism. *Annu. Rev. Biochem.* 2001; 70: 369–413.
- [10] Depowski PL, Rosenthal SI, Brien TP, et al. Topoisomerase II alpha expression in breast cancer: correlation with outcome variables. *Mod Pathol.* 2000; 13: 542–547.
- [11] Villman K, Ståhl E, Liljegren G, Tidefelt U, Karlsson MG. Topoisomerase II-alpha expression in different cell cycle phases in fresh human breast carcinomas. *Mod Pathol.* 2002; 15(5): 486-491.
- [12] Nitiss JL. Targeting DNA topoisomerase II in cancer chemotherapy. *Nature Reviews Cancer.* 2009; 9: 338–350.
- [13] Drake FH, Hoffmann GA, Mong SM, Bartus JO, Hertzberg RP, Johnson RK, Mattern MR, Mirabelli CK. *In vitro* intracellular inhibition of topoisomerase II by the antitumor agent merbarone. *Cancer Res.* 1989; 49(10): 2578-2583.
- [14] Pommier Y, Leo E, Zhang H, Marchand C. DNA topoisomerases and their poisoning by anticancer and antibacterial drugs. *Chem. Biol.* 2010; 17(5): 421-433.
- [15] Jain CK, Majumdera HK, Roy Choudhury BS. Natural Compounds as Anticancer Agents Targeting DNA Topoisomerases. *Current Genomics.* 2017; 18(1): 75-92.
- [16] Pommier Y. Topoisomerase I inhibitors: camptothecins and beyond. *Nat. Rev. Cancer.* 2006; 6(10): 789-802.
- [17] Baikar S, Malpathak N. Secondary metabolites as DNA topoisomerase inhibitors: A new era towards designing of anticancer drugs. *Pharmacognosy Review.* 2010; 4(7): 12-26.

- [18] Bailly C. Contemporary challenges in the design of topoisomerase II inhibitors for cancer chemotherapy. *Chem. Rev.* 2013; 112(7): 3611-3640.
- [19] Pommier Y. Drugging topoisomerases: lessons and challenges. *ACS Chem. Biol.* 2013; 8(1): 82-95.
- [20] Desai AG, Qazi GN, Ganju RK, El-Tamer M, Singh J, Saxena AK, Bedi YS, Aneja SC, Bhat HK. Medicinal plants and Cancer Chemoprevention. *Curr Drug Metab.* 2008; 9(7): 581-591.
- [21] Souza NC, Oliveira JM, Morrone MS, Albanus RD, Amarante MSM, Camillo CS, Langassner SMZ, Gelain DPG, Moreira JCF, Dalmolin RJS, Pasquali MAB. Antioxidant and Anti-Inflammatory Properties of *Anacardium occidentale* Leaf Extract. *Evidence-Based Complementary and Alternative Medicine.* 2017 Jan 1: 2017
- [22] Guzman M. Cannabinoids: potential anticancer agents. *Nat Rev Cancer.* 2003; 3: 745-55.
- [23] Velasco G, Sánchez C, Guzmán M. Towards the use of cannabinoids as antitumour agents. *Nat Rev Cancer.* 2012; 12: 436–444.
- [24] Zhang Y. I-TASSER server for protein 3D structure prediction. *BMC Bioinformatics.* 2008; 9: 40.
- [25] Li H, Leung KS, Wong MH, Ballester PJ. Correcting the impact of Docking pose generation error on binding affinity prediction. *BMC Bioinformatics.* 2016; 17(11): 308.
- [26] Lipinski CA, Lombardo F, Dominy BW, Feeney PJ. Experimental and computational approaches to estimate solubility and permeability in drug discovery and development. *Advanced Drug Delivery Reviews.* 2001; 46: 3–26.
- [27] Wendorff TJ, Schmidt BH, Heslop P, Austin CA, Berger JM. The Structure of DNA-bound human topoisomerase II alpha: conformational mechanisms for coordinating inter-subunit interactions with DNA cleavage. *Journal of molecular biology.* 2012; 424(3-4): 109-24.